RESEARCH ARTICLE

Human papillomavirus type 16 E6 and E7 expression drives transcription of p14(ARF) and p16(INK4a) prior to intragenic methylation of CDKN2A.

Authors

Miriam M. Ben-Dayan[1], Daniel Li[1], Nicole Kawachi[1], Thomas J. Ow[1,2], Thomas J. Belbin[1,3], Geoffrey Childs[1], Nicolas F. Schlecht[1,4,5,6], and Michael B. Prystowsky[1]

Affiliations

[1]Department of Pathology, Albert Einstein College of Medicine, Montefiore Medical Center, Bronx, New York, USA

[2]Department of Otorhinolaryngology-Head and Neck Surgery, Albert Einstein College of Medicine, Montefiore Medical Center, Bronx, New York, USA

[3] Department of Oncology, Memorial University of Newfoundland, Newfoundland and Labrador, Canada

[4]Department of Epidemiology & Population Health, Albert Einstein College of Medicine, Montefiore Medical Center, Bronx, New York, USA

[5]Department of Cancer Prevention & Control, Roswell Park Comprehensive Cancer Center, Buffalo, New York, USA

[6]Faculty of Dentistry, McGill University, Montreal, Canada of Pittsburgh Medical Center, Presbyterian Hospital, Heart and Vascular Institute.

Correspondence

Miriam Ben-Dayan

Department of Pathology, Albert Einstein College of Medicine, Montefiore Medical Center, Bronx, New York, USA
Email: miriam.ben-dayan@einsteinmed.org

Abstract

Human papillomavirus (HPV) positive oropharyngeal squamous cell carcinomas, associated with improved patient outcome, exhibit increased expression of the cyclin dependent kinase inhibitor 2A (*CDKN2A*) tumor suppressor p16(INK4a), while inactivation of the *CDKN2A* locus is frequently observed in HPV negative head and neck squamous cell carcinoma. We recently identified a novel region of intragenic DNA hypermethylation within the *CDKN2A* locus that correlates with RNA expression of two *CDKN2A* transcripts and improved patient outcome in oropharyngeal and laryngeal squamous cell carcinomas. Given the importance of *CDKN2A* expression in HPV-positive oropharyngeal squamous cell carcinoma, we chose an *in vitro* model using primary keratinocytes transduced with HPV type 16 oncogenes *E6* and *E7* to study the relationship between *CDKN2A* methylation and expression. RNA levels for *CDKN2A* transcripts, p14(ARF) and p16(INK4a), as well as keratinocyte differentiation markers and HPV type 16 oncogenes were assessed by real time reverse transcriptase-PCR in the primary cells and after transduction with *E6* and *E7* at two time points. Intragenic *CDKN2A* methylation status, before and after transduction, was determined by the Methylation Sensitive High Resolution Melting Assay followed by sequencing. High levels of HPV oncogene expression lead to an increase in both *CDKN2A* transcription and intragenic methylation. However, *CDKN2A* expression increased early post-transduction, while there was a clear delay in intragenic methylation. Methylation eventually increased suggesting that intragenic methylation is not required for transcription at the *CDKN2A* locus, and that methylation may be a consequence of open and active chromatin.

Keywords: CDKN2A, p16, HPV, HNSCC, DNA methylation, transcription

1. Introduction

Human papillomavirus (HPV) positive head and neck squamous cell carcinoma (HNSCC) has been established as a disease with separate etiology and distinct pathologic and molecular characteristics from HPV-negative HNSCC [1-3], and we have previously shown a decrease of genotypic variation at the RNA level among HPV-positive oropharyngeal squamous cell carcinomas (OPSCC) [4]. HPV infection (primarily with the high-risk serotypes, HPV-16 and HPV-18) drives carcinogenesis via the action of the E6 and E7 oncoproteins, which respectively inhibit the tumor suppressors, p53 and Retinoblastoma (Rb) (**Figure 1**). HPV-positive OPSCC is strongly associated with high tumor cell expression of p16, which, along with the p14 protein, are the main products of the cyclin dependent kinase inhibitor 2A (*CDKN2A*) gene. Immunostaining for p16 is commonly used as a surrogate marker for HPV infection in OPSCC. Clinically, HPV infection in OPSCC is associated with improved response to therapy and patient survival [1,3]; p16 expression has been established as an independent prognostic factor for survival in OPSCC [1], and has been reported to be associated with improved

outcomes in HPV-positive non-oropharyngeal HNSCC [5,6]. Though HPV has been implicated as a growing cause of HNSCC, the molecular events that occur during the complex process of HPV-mediated carcinogenesis in OPSCC are not fully understood.

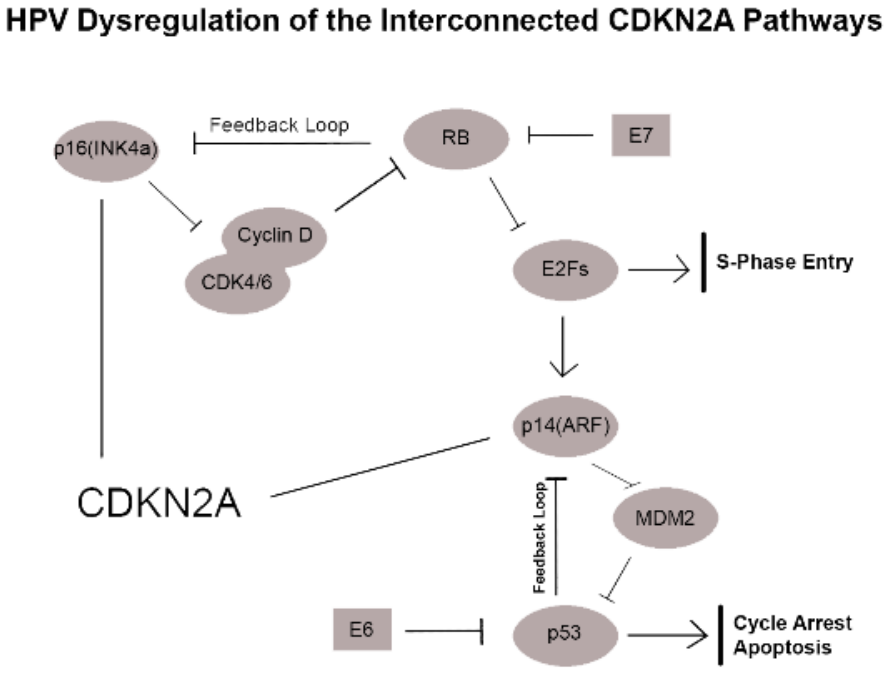

Figure 1: *HPV oncogenes E6 and E7 disrupt the interconnected p14(ARF) and p16(INK4a) pathways.* To avoid apoptosis and ensure continued cellular proliferation, HPV-16 oncogenes *E6* and *E7* inhibit p53 and *RB*. The CDKN2A transcript p16(INK4a) is an upstream member of the *RB* pathway, and is upregulated via a negative feedback loop with *RB* and aberrant proliferative signals. CDKN2A transcript p14(ARF) is an upstream member of the p53 pathway but it is also a downstream member of the *RB* pathway, thus connecting the *RB* and p53 pathways. The p14(ARF) transcript is upregulated by E2Fs and via a negative feedback loop with p53. In cells expressing HPV-16 *E6* and *E7*, p53 and *RB* expression remains low, sending feedback signals for CDKN2A transcription.

HPV-negative and HPV-positive HNSCC are molecularly and biologically distinct. Both forms of HNSCC exhibit fundamental disruption of key tumor suppressors and cell cycle regulators, albeit via very different mechanisms [7]. Most HPV-negative HNSCCs lose expression of p16 via deletion or silencing of *CDKN2A* and lose p53 function via mutation of the tumor protein p53 (*TP53*) gene. In comparison, the *CDKN2A* and *TP53* genes remain intact in HPV-positive OPSCC since p53 and Rb function are disrupted via E6 and E7 activity, and *CDKN2A* transcripts have been demonstrated to be overexpressed in HPV-positive disease [8,9], including OPSCC [10]. Global methylation events, known to be significantly altered in cancer cells, also appear to differ between HPV-positive and HPV-negative HNSCCs. Work by our group [11] and others [12,13] describe major differences in DNA methylation patterns between HPV-positive and HPV-negative HNSCCs. The expression of HPV oncogenes alters methylation of the viral and the host genome [14] via the indirect

upregulation of DNA methyltransferase I (DNMT1) by E6 [15] and direct stimulation of DNMT1 activity by E7 [16]. Thus, the global methylation changes seen in HPV-positive HNSCC may be due to aberrant DNMT1 expression and activity.

Most work examining DNA methylation changes in cancer has focused on the hypermethylation of CG dinucleotide (CpG) enriched regions, also known as CpG islands, in promotor regions and the role of gene silencing in the process of carcinogenesis [17]. However, hypermethylation of CpG islands within the gene body, both exonic and intronic, have also been shown to alter gene expression [18,19]. The function of intragenic methylation is poorly understood, though some hypothesize that it may increase efficiency of transcription elongation by repressing spurious intragenic transcription [20], or it may play a role in the regulation of gene splicing when methylation sites occur at exon-intron boundaries [18]. Within the *CDKN2A* locus, exon 2 methylation has been shown to decrease p16(INK4a) expression, and it is being studied as a possible prognostic biomarker in esophageal cancer [21] and colorectal cancer [22], and this methylation signature is also associated with carcinogenesis in breast cancer [23] and cervical cancer [24]. Conversely, in a mouse model of hepatocellular cancer evaluating methylation and expression across several genes, intragenic *CDKN2A* hypermethylation was associated with increased expression, although the study included all intragenic CpG islands, not just the CpG island found at exon 2 [25]. Evidently, the relationship between methylation and *CDKN2A* expression in HNSCC deserves further examination.

Our previous work demonstrated that HPV-positive tumors have a significantly higher number of methylated CpG loci compared to those that are HPV-negative [11], including a cluster of non-promoter CpG sites located at an intronic CpG island within the *CDKN2A* gene (**Figure 2**). Our validation studies also demonstrated that hypermethylation of the *CDKN2A*-specific loci in HPV-positive OPSCC were associated with increased expression of *CDKN2A* gene products (p16INK4a and p14ARF), and, not surprisingly, these molecular characteristics were associated with improved survival [10]. Interestingly, a follow-up study of *CDKN2A* methylation and transcript expression demonstrated the same relationship was associated with survival in a cohort of patients with laryngeal squamous cell carcinoma, which were largely HPV-negative [26]. These results have led to several new questions regarding the relationship between HPV infection and carcinogenesis in HNSCC. Specifically, it is unclear if there is a causal link between HPV infection and methylation of the *CDKN2A* CpG sites. Additionally, since the CpG islands in *CDKN2A* were not located in the promoter region, it is not known whether methylation of these sites contribute to or control expression of the *CDKN2A* transcripts. Given the importance of p16 expression in the diagnosis and prognosis of HPV-positive OPSCC, we have sought to explore the relationship between nonpromoter methylation and CDKN2A transcription. Here, we demonstrate an *in vitro* approach to investigate this question by transfecting human keratinocytes with HPV-16 oncogenes *E6* and *E7* and investigating the temporal relationship between CDKN2A methylation and transcription.

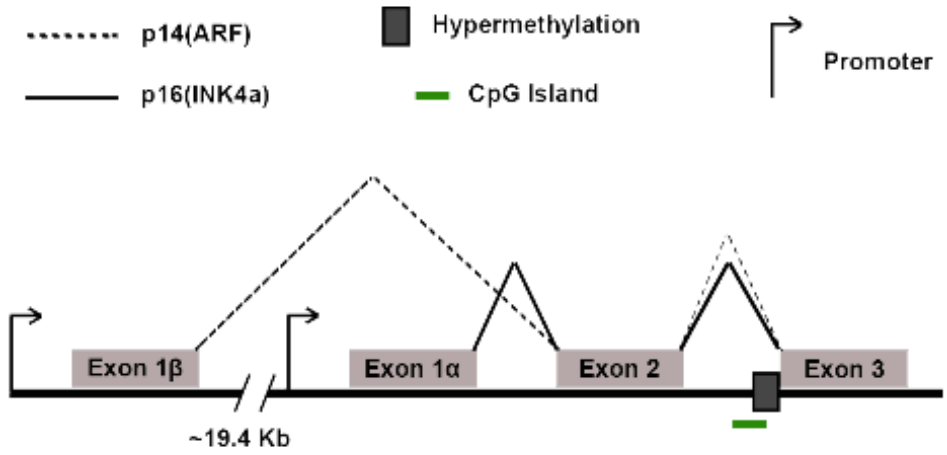

Figure 2: *Map of the CDKN2A locus showing the previously described region of non-promoter hypermethylation.* Map of the CDKN2A locus which encodes tumor suppressors p14(ARF) and p16(INK4a). Both transcripts share CDKN2A exons 2 and 3, but they each have unique first exons and promoter regions, as shown. Predicted CpG Islands are located at each promoter, across the entire exon 2, and immediately before exon 3 (shown as a green bar). We previously described a region of CDKN2A non-promoter hypermethylation that is associated with p14(ARF) and p16(INK4a) expression in primary oropharyngeal and laryngeal tumors. The hypermethylated region (shown as a dark grey box) overlaps with the CpG Island located directly upstream of exon 3.

2. Materials and Methods

2.1 Tissue Culture

Two vials of single donor primary foreskin normal Human Epidermal Keratinocytes (referred to as HEKe and HEKn in this paper) were purchased from Gibco® (Invitrogen, Carlsbad, CA). Primary HEK cells were grown in Gibco® EpiLife™ Medium supplemented with Gibco® Human Keratinocyte Growth Supplement and Gibco® Penicillin-Streptomycin (Invitrogen, Carlsbad, CA). As a control, the HPV16-positive oral keratinocyte cell line HOK16B (courtesy of Dr. No-Hee Park, UCLA school of dentistry) was grown in Gibco® EpiLife™ Medium supplemented with Gibco® Human Keratinocyte Growth Supplement, Gibco® Penicillin-Streptomycin, and Gibco® 5% Fetal Bovine Serum (Invitrogen, Carlsbad, CA). All plates were coated with the Gibco® Coating Matrix Kit Protein according to the manufacturer's instructions (Invitrogen, Gaithersburg, MD).

Fresh medium was added to all cell types every other day. All cells were passaged at 80% confluency using Gibco® TrypLE™ Express Enzyme (1X) without phenol red (Invitrogen, Carlsbad, CA). HEKe and HEKn cells were pelleted at 100xg for 5 minutes before plating. Medium containing serum was used to dilute the TrypLE solution before plating the HOK16B cells.

2.2 Retroviral Transductions

The retroviral packaging line PA317 LXSN 16E6E7 was purchased from the American Type Culture Collection (ATCC; Manassas, VA). Cells were centrifuged at 125xg for 5 minutes and plated immediately upon arrival. Cells were grown in Gibco® DMEM low glucose, pyruvate medium supplemented with Gibco® Penicillin-

Streptomycin and Gibco® 10% Fetal Bovine Serum (Invitrogen, Carlsbad, CA). Viral collection was done at 24 and 48 hours after plating. The collected viral medium was filtered using a Steriflip® 0.22µm Millipore Express® Plus Membrane (Millipore, Burlington, MA). The collected retrovirus was aliquoted and stored at -80˚C.

To prepare for retroviral transductions, primary HEKe cells were plated at a density of 100,000 cells per well on a 6-well Corning™ Costar™ Flat Bottom Cell Culture plate (Corning, Corning, NY). Serum free EpiLife™ medium was replaced by filtered viral medium 24 hours after plating. HEKe cells were treated with 10µg/mL of polybrene, and the plates were rocked gently for 2 hours at 37˚C. Fresh serum free EpiLife™ medium was then added to each well, and the cells were incubated at 37˚C overnight. The retrovirus containing medium was removed the next day, and fresh serum free EpiLife™ medium was added to each well. Only one newly transduced cell line (HEKe E6E7) survived the polybrene treatment. Once the HEKe E6E7 cells grew to 70% confluency, they were passaged and expanded.

Retroviral transductions were also done for primary HEKn cells. After viral medium was added, the HEKn cells were treated with 8µg/mL of polybrene, and the plates were incubated at 37˚C for two hours with frequent rocking. Viral containing medium was replaced with fresh serum free EpiLife® medium, and the cells were incubated at 37˚C overnight. Four cell lines were generated with this method (HEKn E6E7 A, HEKn E6E7 B, HEKn E6E7 C, and HEKn E6E7 D). Once the cells grew to 70% confluency, serum free EpiLife™ medium supplemented with 200µg/mL of G418 Sulfate (Corning, Corning, NY) was added to select for successful transduction. Selection medium was used for a total of 5 days. The surviving cells were transferred to a larger plate and expanded once they reached 70% confluency. Subsequent passaging for all transduced lines was done once the cells reached 80% confluency.

2.3 Montefiore Medical Center Primary Tumors

Primary HPV-positive OPSCC tumors from 8 patients undergoing treatment at Montefiore Medical Center (MMC) in Bronx, NY were used as a biological reference for select genes. The patients used in this study provided written consent under a protocol approved by the Institutional Review Board at MMC. The tumors were snap-frozen in liquid nitrogen and kept frozen at -80˚C until processing. Histological confirmation of the tumors was performed as previously described [11]. Control samples were acquired and used to determine percentage of tumor, degree of necrosis, and lymphocytic infiltration as previously described [27]. HPV status for each tumor was determined by the presence of DNA from the HPV L1 region and expression of HPV16 oncogenes E6 and E7 [28].

2.4 RNA Collection and Expression Analysis

Total RNA was collected for primary HEK cells, HEKe E6E7 cells, HEKn E6E7, and HOK16B cells using the RNeasy Mini Kit (QIAGEN, Hilden, Germany) according to the manufacturer's protocol. All cells were grown to 80% confluency before RNA extraction. RNA extractions were done for three flasks of primary HEKe and HEKn cells at passage 5 as a negative control, and three flasks of HOK16B cells as a positive control. Extractions were done for three flasks of HEKe E6E7 cells at passages 2 (HEKe E6E7 P2) and 7 (HEKe E6E7 P7) after transductions. RNA was extracted for one flask of each HEKn E6E7 cell line at

passages 5 (HEKn E6E7 P5) and 10 (HEKn E6E7 P10) after transductions.

RNA expression levels for the p14(ARF), p16(INK4a), involucrin (*IVL*), keratin 14 (*KRT14*), HPV-16 *E6*, HPV-16 *E7*, and glyceraldehyde 3-phosphate dehydrogenase (*GAPDH*) genes were quantified for all cells grown by real time reverse transcriptase-PCR (qRT-PCR). In addition, expression levels for the p14(ARF), p16(INK4a), HPV-16 *E6*, and HPV-16 *E7* genes were quantified for the 8 primary HPV-positive oropharyngeal tumors. Taqman® qRT-PCR probes were used with the TaqMan® RNA-to-Ct™ 1-Step Kit (Applied Biosystems, Waltham, MA) for 100ng of total RNA to obtain cycle threshold (CT) values. All CT values were normalized to *GAPDH* and subsequently converted to Median Fold-Difference ($2^{-\Delta\Delta CT}$) values.

2.5 DNA Collection and Methylation Analysis

DNA was collected for all cells grown using the DNeasy Blood & Tissue Kit (QIAGEN, Hilden, Germany) according to the manufacturer's protocol. DNA extractions were done in parallel with RNA extractions, so that passage number and cell confluency remained consistent between the two experiments.

Methylation was assessed by the Methylation Sensitive High Resolution Melting (MS-HRM) protocol [29] as well as subsequent sequencing. For this experiment, methylation status for the previously described *CDKN2A* intragenic region [10] was done using two overlapping primer sets (Primer Set 1: (F) 5'-TCGGAAATTATTTGTGGGTTTGTAGAAGTA-3' and (R) 5'-TTCCCGCATCCCCAAACATCTTTTA-3'; Primer Set 2: (F) 5'-TTTTTAAGTGTAAATGTTGTTTCGGGAGAAT-3' and (R) 5'-GATAACCAAAAAACGCCTCAAACTCTAA-3'). DNA was bisulfite converted using the EZ DNA Methylation Gold Kit (Zymo Research, Irvine, CA) and percent methylation was determined with the LightCycler® 480 High Resolution Master Kit (Roche, Indianapolis, Indiana) according to the manufacturer's protocol. Products from the MS-HRM assay were then sent for sequencing.

3. Results

3.1 Stable cell lines expressing HPV-16 oncogenes E6 and E7 were created from primary HEK cells

Previously, we found that increased expression of p16(INK4a) and p14(ARF), two transcript variants from the *CDKN2A* gene, correlated with methylation of nonpromoter regions of the *CDKN2A* gene in both HPV-positive oropharyngeal squamous cell cancers and in laryngeal squamous cell cancers regardless of HPV infection [10,26]. To determine if nonpromoter methylation was required for expression of *CDKN2A* gene transcripts or if HPV-16 oncogenes *E6* and *E7* could drive *CDKN2A* transcription without methylation, we transduced primary human foreskin keratinocytes from two separate donors (HEKe and HEKn) with a retrovirus containing both HPV-16 oncogenes. One HEKe E6E7 cell line and four HEKn E6E7 cell lines were created with the transduction method. DNA and RNA were collected in triplicate for the cells that survived the transduction at two time points, with five passages in between collections. The primary keratinocytes stopped dividing and displayed a differentiated keratinocyte morphology in a smaller number of passages than the transduced lines (data not shown), which were maintained for 15 passages post-transduction and then frozen for future use.

HPV-16 oncogene RNA expression was then assessed by qRT-PCR for the primary HEKe cells, the primary HEKn cells, the HEKe E6E7 line, the HEKn E6E7 lines, and an HPV16-positive oral keratinocyte cell line (HOK16B). HPV-16 *E6* and *E7* expression for HOK16B, shown as the mean ΔCT (n=3), was calculated using *GAPDH* as the reference gene. HOK16B was then set as the baseline (value of 1) for the Median Fold-Difference calculations of viral RNA levels for the HEKe E6E7 (n=3) and HEKn E6E7 (n=4) lines at two time points (**Table 1**). The primary HEKe and HEKn cells did not express *E6* or *E7* (data not shown). At all of the time points, both HEKe E6E7 and HEKn E6E7 expressed *E6* and *E7* at higher levels than observed in HOK16B, shown as the Median Fold-Increase. These data show that we successfully created stable *E6* and *E7* expressing HEK cell lines. In addition, we also assessed the RNA expression of *E6* and *E7* for 8 primary HPV-positive OPSCC tumors obtained from MMC MMC Primary Tumors). HOK16B was again used as a reference for expression in the Median Fold-Difference calculations, shown as the Median Fold-Increase. Primary tumor median RNA levels for both *E6* and *E7* were closer to reference HOK16B levels compared to the transduced HEKe and HEKn lines.

	HOK16B		HEKe E6E7 P2		HEKe E6E7 P7		HEKn E6E7 P5		HEKn E6E7 P10		MMC Primary Tumors	
Genes	*Mean ΔCT*	*SD*	*Median Fold-Increase*	*CV*	*Median Fold-Increase*	*CV*	*Median Fold-Increase*	*CV*	*Median Fold-Increase*	*CV*	*Median Fold-Increase*	*CV*
HPV-16 E6	-3.5	0.22	5.0	0.37	10.8	0.09	5.8	0.64	3.1	0.42	1.7	1.78
HPV-16 E7	-2.0	0.22	5.2	0.36	10.5	0.09	3.6	0.67	2.5	0.42	0.8	1.66

Table 1: *High levels of HPV-16 oncogenes E6 and E7 are observed for transduced HEKe and HEKn cells at the first time point post-transduction.* RNA expression for HPV-16 oncogenes *E6* and *E7* was determined by qRT-PCR for the HOK16B line, the HEKe E6E7 line at two time points, the HEKn E6E7 line at two time points, and 8 primary HPV-positive oropharyngeal tumors (MMC Primary Tumors). The HOK16B line was used as a baseline for expression (value of 1). HOK16B RNA levels are shown as mean ΔCT (n=3), and they were calculated using *GAPDH* as the reference gene. The standard deviation (SD) is shown for baseline expression levels. Median Fold-Increases from baseline were then calculated for HEKe E6E7 P2 (n=3), HEKe E6E7 P7 (n=3), HEKn E6E7 P5 (n=4), HEKn E6E7 P10 (n=4), and MMC Primary Tumors (n=8). Coefficients of variation (CV; σ/μ) are shown for all Median Fold-Increase values. We observed high levels of HPV-16 *E6* and *E7* for HEKe E6E7 and HEKn E6E7 lines at both time points, suggesting that we successfully created stable cell lines.

3.2 Baseline host gene RNA levels were established to determine Fold-Changes in expression

Having established HEKe E6E7 and HEKn E6E7 cell lines, we wanted to assess the time dependence of expression of multiple host genes using qRT-PCR and primary HEK cells as a baseline for expression when compared to expression in HEKe E6E7 line, HEKn E6E7 lines, and HOK16B. In addition to p14(ARF) and p16(INK4a), we also chose to include keratinocyte differentiation markers *KRT14* (keratin 14, a marker for undifferentiated keratinocytes) [30] and *IVL* (involucrin, a marker for terminally differentiated keratinocytes) [30] as well as *GAPDH* (glyceraldehyde 3-phosphate dehydrogenase, a housekeeping gene).

Host gene expression was then assessed for the primary HEKe cells, the primary HEKn cells, the HEKe E6E7 line, the HEKn E6E7 lines, and the HOK16B cells (**Tables 2-3**). Expression for the primary HEKe and HEKn cells, shown as mean ΔCT (n=3), was calculated using GAPDH as the reference gene. Primary HEKe expression was then set as the baseline (value of 1) for the Median Fold-Change (n=3) calculations of host genes for the two HEKe E6E7 times points. Similarly, primary HEKn expression was set as the baseline (value of 1) for the Median Fold-Change (n=4) calculations of host genes for the two HEKn E6E7 time points. The Median Fold-Difference (n=3) of host gene expression for the HOK16B line was calculated with both the HEKe basline and the HEKn baseline.

3.3 Keratinocyte differentiation markers were used to assess differentiation after transduction

Differentiation marker *KRT14* is expressed in the proliferative basal layer of the stratified squamous epithelium [31], conversely, *IVL* is expressed in cells that have left the basal layer and have stopped dividing [32]. Primary keratinocytes growing in culture will contain a population of terminally differentiated keratinocytes expressing *IVL* [33]. However, since HPV-16 oncogene expression suppresses cellular differentiation and suspends keratinocytes in a proliferative state [34-36], we expected to see high levels of *KRT14* and decreased levels of *IVL* due to a decreasing population of differentiated cells (**Table 2**). The baseline ΔCT values for the primary cells were used to determine the initial differentiation level for each group of cells. At baseline, both primary HEKe and HEKn cells had levels of *KRT14* that were higher than *GAPDH*, indicated with a positive ΔCT value. Despite the slight decrease of *KRT14* in the HEKe E6E7 and HEKn E6E7 lines, both transduced lines retained levels of *KRT14* that were higher than *GAPDH*. Conversely, the Median Fold-Change, shown as the Median Fold-Decrease, for *IVL* decreased for both the HEKe E6E7 and HEKn E6E7 lines by the second time point. The Median Fold-Decrease for HOK16B *IVL* RNA levels are well below the baseline levels observed for the primary keratinocytes suggesting that long term maintenance of the transductants might result in further decrease in *IVL* levels. Together, the *KRT14* and *IVL* levels in the transduced lines support that the cells remained undifferentiated at the last RNA collection.

	Baseline Primary HEKe							
	Primary HEKe		HEKe E6E7 P2		HEKe E6E7 P7		HOK16B	
Genes	*Mean ΔCT*	*SD*	*Median Fold-Decrease*	*CV*	*Median Fold-Decrease*	*CV*	*Median Fold-Decrease*	*CV*
KRT14	2.1	0.5	1.1	0.06	1.4	0.11	5.8	0.07
IVL	-6.9	1.67	-1.3	0.23	4.2	0.24	67.8	0.11
	Baseline Primary HEKn							
	Primary HEKn		HEKn E6E7 P5		HEKn E6E7 P10		HOK16B	
Genes	*Mean ΔCT*	*SD*	*Median Fold-Decrease*	*CV*	*Median Fold-Decrease*	*CV*	*Median Fold-Decrease*	*CV*
KRT14	2.0	0.46	1.0	0.2	1.8	0.07	5.5	0.07
IVL	-6.9	0.49	3.5	0.2	2.3	1.4	69.7	0.11

Table 2: *RNA levels for KRT14 remained high and RNA levels for IVL remained low at two time points post-transduction with HPV-16 E6 and E7.* RNA expression for *KRT14* and *IVL* was determined by qRT-PCR for the HEKe E6E7 and HEKn E6E7 lines at two time points. RNA expression for both genes was also determined by the same method for the HOK16B line for reference. The primary HEKe and HEKn cells were used as a baseline of expression (value of 1) for their respective transduced lines. Primary HEKe and HEKn RNA levels are shown as mean ΔCT (n=3), and they were calculated using *GAPDH* as the reference gene. The standard deviation (SD) is shown for baseline expression levels. The Median Fold-Decrease from the primary HEKe baseline was then calculated for HEKe E6E7 P2 (n=3) and HEKe E6E7 P7 (n=3), and the Median Fold-Decrease from the primary HEKn baseline was calculated for HEKn E6E7 P5 (n=4), and HEKn E6E7 P10 (n=4). Median Fold-Decreases from each baseline were also calculated for the HOK16B line (n=3). Coefficients of variation (CV; σ/μ) are shown for all Median Fold-Decrease values. Despite seeing a decrease in *KRT14* in the transduced lines, *KRT14* levels remained above *GAPDH* expression at the second time point. We observed high levels of *KRT14* and low levels of *IVL* for HEKe E6E7 and HEKn E6E7 lines at both time points. These data support minimal, if any, keratinocyte differentiation throughout our experiments.

3.4 Transduced HEK cells exhibit increased CDKN2A expression at early passages

We then assessed the baseline RNA levels of p14(ARF) and p16(INK4a) for the primary keratinocytes (**Table 3**). At baseline, the p14(ARF) and p16(INK4a) RNA levels were lower than HOK16B for the primary HEKe and HEKn cells. Both p14(ARF) and p16(INK4a) exhibited an increase in expression, shown as Median Fold-Increase, for the HEKe E6E7 and the HEKn E6E7 lines at the first time point. The Median Fold-Change, shown as the Median Fold-Increase, of p14(ARF) and p16(INK4a) for the HEKe E6E7 line appears to increase with passage number, while only p14(ARF) shows this trend for the HEKn E6E7 lines. The Median Fold-Increase for the HOK16B line and the primary HPV-positive oropharyngeal tumors (n=8) are shown for reference.

	Baseline Primary HEKe									
	Primary HEKe		HEKe E6E7 P2		HEKe E6E7 P7		HOK16B		MMC Primary Tumor	
Genes	*Mean ΔCT*	*SD*	*Median Fold-Increase*	*CV*	*Median Fold-Increase*	*CV*	*Median Fold-Increase*	*CV*	*Median Fold-Increase*	CV
p14(ARF)	-10.3	0.15	7.3	0.12	16.4	0.04	29.5	0.44	6.4	1.28
p16(INK4a)	-10.6	0.25	31.1	0.1	71.3	0.21	92.4	0.47	7.8	1.28
	Baseline Primary HEKn									
	Primary HEKn		HEKn E6E7 P5		HEKn E6E7 P10		HOK16B		MMC Primary Tumor	
Genes	*Mean ΔCT*	*SD*	*Median Fold-Increase*	*CV*	*Median Fold-Increase*	*CV*	*Median Fold-Increase*	*CV*	*Median Fold-Increase*	CV
p14(ARF)	-10.1	0.44	4.0	0.28	5.4	0.16	24.9	0.44	5.4	1.28
p16(INK4a)	-6.8	0.15	8.7	0.47	6.8	0.16	6.7	0.47	0.6	1.26

Table 3: *RNA expression for both p14(ARF) and p16(INK4a) increase for HEKe E6E7 and HEKn E6E7 lines early after transduction with HPV-16 E6 and E7.* RNA expression for p14(ARF) and p16(INK4a was determined by qRT-PCR for the HEKe E6E7 and HEKn E6E7 lines at two time points. RNA expression for both *CDKN2A* transcripts was also determined by the same method for the HOK16B line and 8 primary HPV-positive oropharyngeal tumors for reference. The primary HEKe and HEKn cells were used as a baseline of expression (value of 1) for their respective transduced lines. Primary HEKe and HEKn RNA levels are shown as mean ΔCT (n=3), and they were calculated using *GAPDH* as the reference gene. The standard deviation (SD) is shown for baseline expression levels. The Median Fold-Increase from the primary HEKe baseline was then calculated for HEKe E6E7 P2 (n=3) and HEKe E6E7 P7 (n=3), and the Median Fold-Increase from the primary HEKn baseline was calculated for HEKn E6E7 P5 (n=4), and HEKn E6E7 P10 (n=4). Median Fold-Increases from each baseline were also calculated for the HOK16B line (n=3) and MMC Primary Tumors (n=8) for reference. Coefficients of variation (CV; σ/μ) are shown for all Median Fold-Increase values. We observed an increase in both p14(ARF) and p16(INK4a) for the HEKe E6E7 and HEKn E6E7 lines at both time points, suggesting an early upregulation of *CDKN2A* transcription post-transduction with HPV-16 *E6* and *E7*.

3.5 CDKN2A methylation is only observed in transduced HEK cells at later passages

As we have shown previously in primary patient tumors [10], there is an association between *CDKN2A* variant expression and *CDKN2A* intragenic CG dinucleotide (CpG) methylation. Once we established that increased *CDKN2A* expression occurs shortly after HPV-16 oncogene expression, we decided to assess the *CDKN2A* methylation status for the HEKe E6E7 and HEKn E6E7 lines. To test the relationship between *CDKN2A* expression and methylation, we used the Methylation Sensitive High Resolution Melting (MS-HRM) assay and subsequent DNA sequencing for the primary HEK cells, HEKe E6E7 line, HEKn E6E7 lines, and HOK16B.

With two overlapping primer sets and multiple standards, we were able to generate MS-HRM curves and approximate percentage of CpG methylation for the *CDKN2A* locus (**Figure 3**). Melting curves for each line were compared to methylation standards of 0%, 5%, 10%, 15%, 25%, 50%, and 100%. The MS-HRM curve for primary HEKe cells aligned with the unmethylated standard curve (data not shown). Likewise, the MS-HRM curve for HEKe E6E7 P2 (green curve) showed 0% methylation (**Figure 3A**). Interestingly, the HEKe E6E7 P7 MS-HRM curve (green curve) aligned with the 25% methylation standard (blue

curve; **Figure 3B**). We observed the same trend with the HEKn cells (**Figure 3C**). Primary HEKn cells exhibited a baseline of approximately 5% methylation, with no detectable change in methylation for HEKn E6E7 P5. As with the HEKe E6E7 line, we did observe approximately 25% methylation for HEKn E6E7 P10. Thus, *CDKN2A* intragenic methylation occurs more slowly after transduction with HP-16 *E6* and *E7* (**Figure 4**) than the increase in *CDKN2A* expression indicating that intragenic methylation is not required for *CDKN2A* transcription.

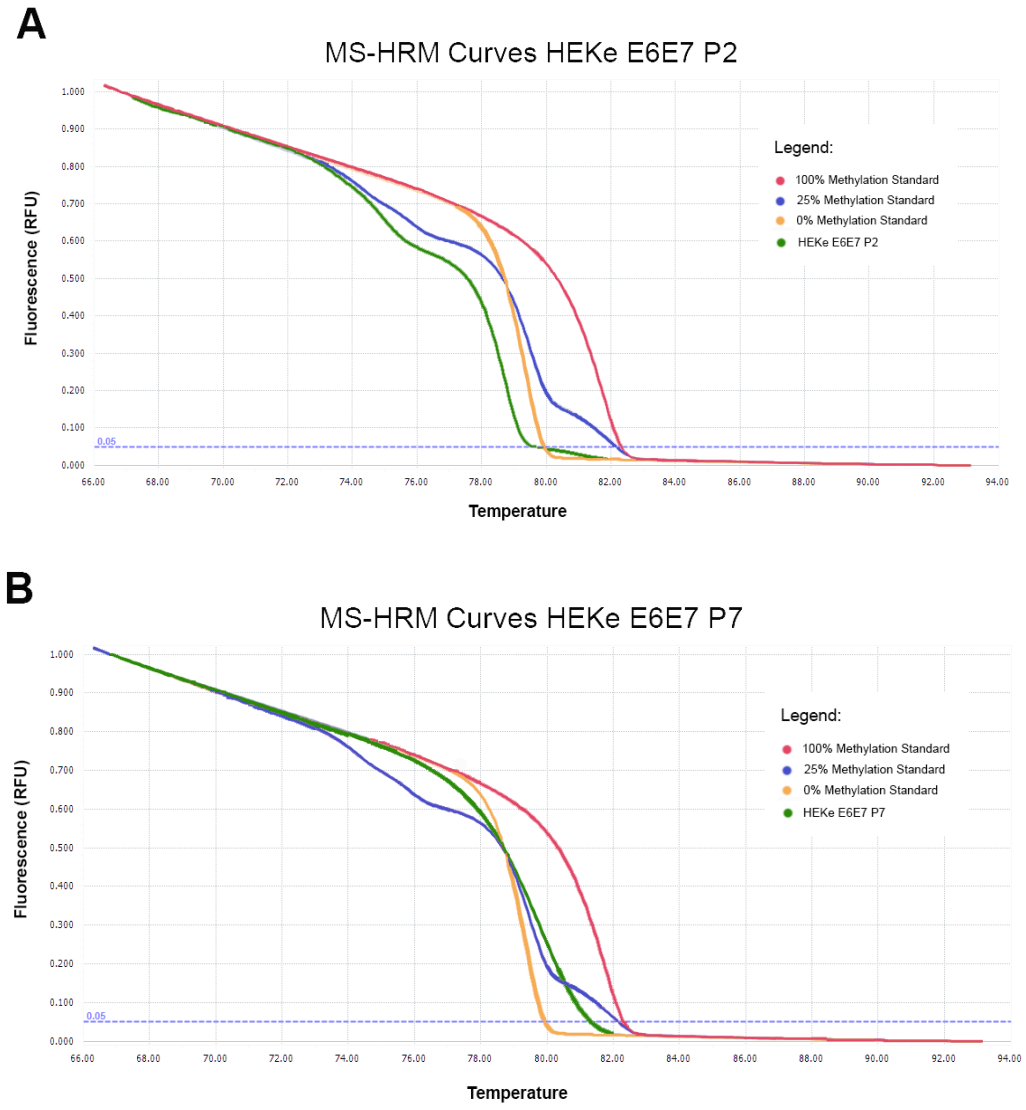

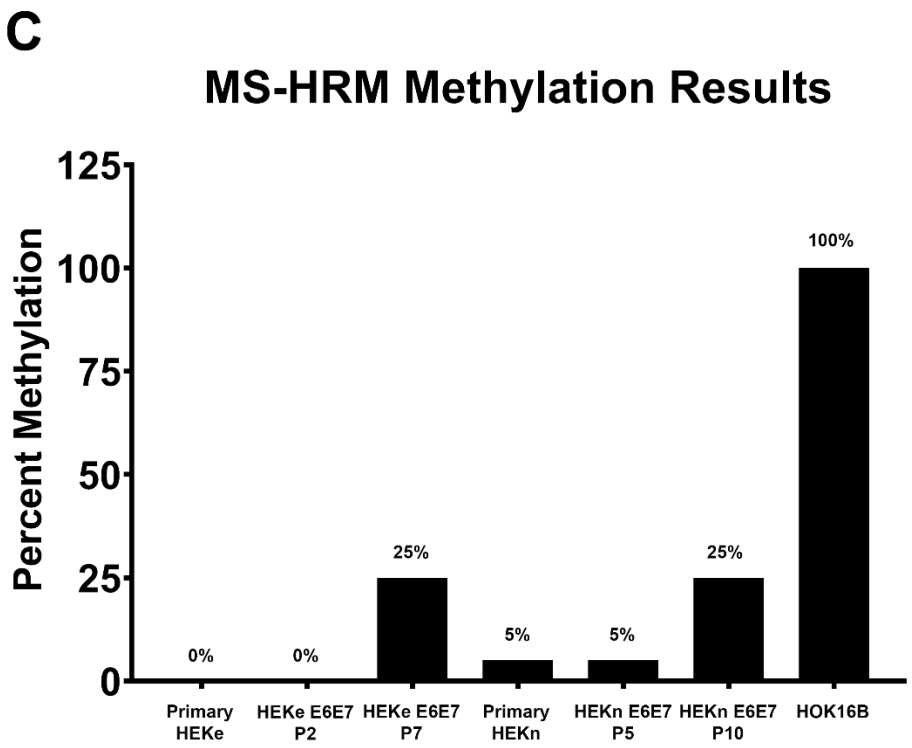

Figure 3: *An increase in CDKN2A intragenic methylation is observed at the second time point after transduction with HPV-16 E6 and E7 for both HEKe and HEKn cells. CDKN2A* methylation status was determined by MS-HRM. Melting curves were generated for bisulfite converted DNA from primary HEK cells, HEKe E6E7, HEKn E6E7, and HOK16B. **3A.** Representative of HEKe E6E7 P2 melting curves for primer set 1 in triplicates. MS-HRM standards shown are 100% methylated (red), 25% methylated (blue), and 0% methylated (yellow). We observed 0% methylation for HEKe E6E7 P2 (green). **3B.** Representative of HEKe E6E7 P7 melting curves for primer set 1 in triplicates. MS-HRM standards shown are 100% methylated (red), 25% methylated (blue), and 0% methylated (yellow). We observed approximately 25% methylation for HEKe E6E7 P7 (green). **3C.** Overall MS-HRM results graphed as percent methylation for each cell type. No methylation was detected with either primer set for primary HEKe cells and HEKe E6E7 P2 (n=3). Primary HEKn cells started with a baseline of 5% methylation (n=3) for both primer sets, and we observed no change in methylation for HEKn E6E7 P5 (n=4). We were able to detect a clear increase in methylation for HEKe E6E7 P7 (n=3) and HEKn E6E7 P10 (n=4), both show approximately 25% methylation based on the standards used for this assay. HOK16B, our HPV-positive control, was 100% methylated (n=3).

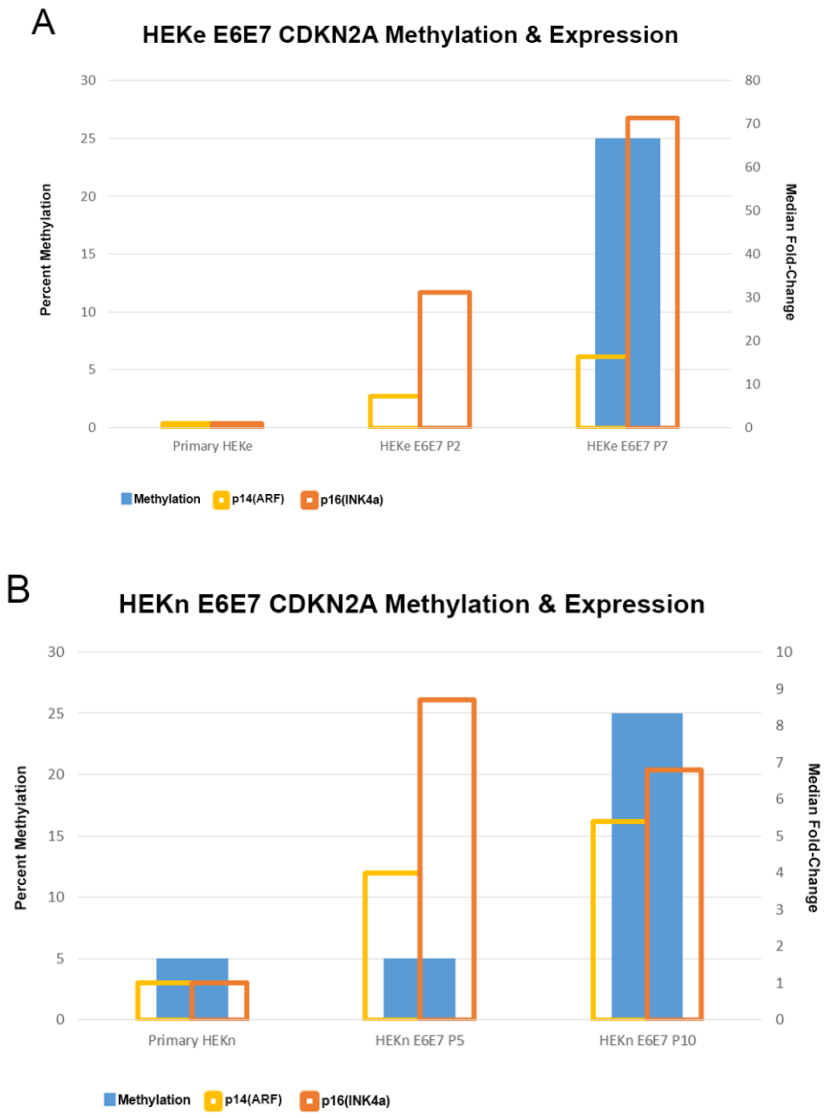

Figure 4: *Increased CDKN2A expression is observed earlier than methylation for both HEKe and HEKn cells post-transduction with HPV16 E6 and E7.* Overlay of *CDKN2A* expression (Median Fold-Change) determined by qRT-PCR and *CDKN2A* methylation status (Percent Methylation) determined by MS-HRM. **4A.** The *CDKN2A* Median Fold-Change for HEKe E6E7 P2 and HEKe E6E7 P7 cells were determined using primary HEKe expression (Mean ΔCT, n=3; *GAPDH* expression – HEKe expression) as a baseline (value of 1). We observed an increase in p14(ARF) and p16(INK4a) expression (yellow and orange bar, respectively) for HEKe E6E7 P2, suggesting increased transcription of *CDKN2A* shortly after transduction with HPV-16 oncogenes. Unlike *CDKN2A* expression, we only observed an increase in *CDKN2A* intragenic methylation (blue bar) for HEKe E6E7 P7, suggesting a delayed response after transduction with HPV-16 oncogenes. **4B.** The *CDKN2A* Median Fold-Change for HEKn E6E7 P5 and HEKn E6E7 P10 cells were determined using primary HEKn expression (Mean ΔCT, n=3; *GAPDH* expression – HEKn expression) as a baseline (value of 1). We observed an increase in p14(ARF) and p16(INK4a) expression (yellow and orange bar, respectively) for HEKn E6E7 P5, suggesting increased transcription of *CDKN2A* shortly after transduction with HPV-16 oncogenes. Unlike *CDKN2A* expression, we only observed a relative increase in *CDKN2A* intragenic methylation (blue bar) for HEKn E6E7 P10, suggesting a delayed response after transduction with HPV-16 oncogenes.

After establishing an approximate percent methylation for *CDKN2A*, we sequenced the products from the MS-HRM assay. Sequencing of the *CDKN2A* intragenic segment of primary HEK, HEKe E6E7, and HOK16B cells, four HEKn E6E7 lines was performed (**Figure 5**). As expected, all of the CpGs in the region of interest for the HOK16B cells were 100% methylated (shown with a black circle). All of the CpGs for both the primary HEKe and HEKe E6E7 P2 cells were 0% methylated (shown with an empty circle), indicating no change after transduction with HPV-16 oncogenes. We did observe methylation for HEKe E6E7 P7, although there was a mixture of 100% methylated CpGs and partially methylated CpGs (shown with a grey circle). The HEKn cells started with some methylation, but the methylation pattern remained the same for HEKn E6E7 P5 cells. Similar to HEKe transduced cells, we observed an increase in methylation for HEKn E6E7 P10 cells, even though we were unable to get sequencing data for a few of the CpGs (shown with a blue circle). These data confirm our MS-HRM results, and *CDKN2A* intragenic methylation occurs after *CDKN2A* RNA expression increases. Interestingly, the methylation patterns for the HEKe E6E7 and HEKn E6E7 lines were highly similar at the second time point, suggesting a predictable pattern of methylation over several passages.

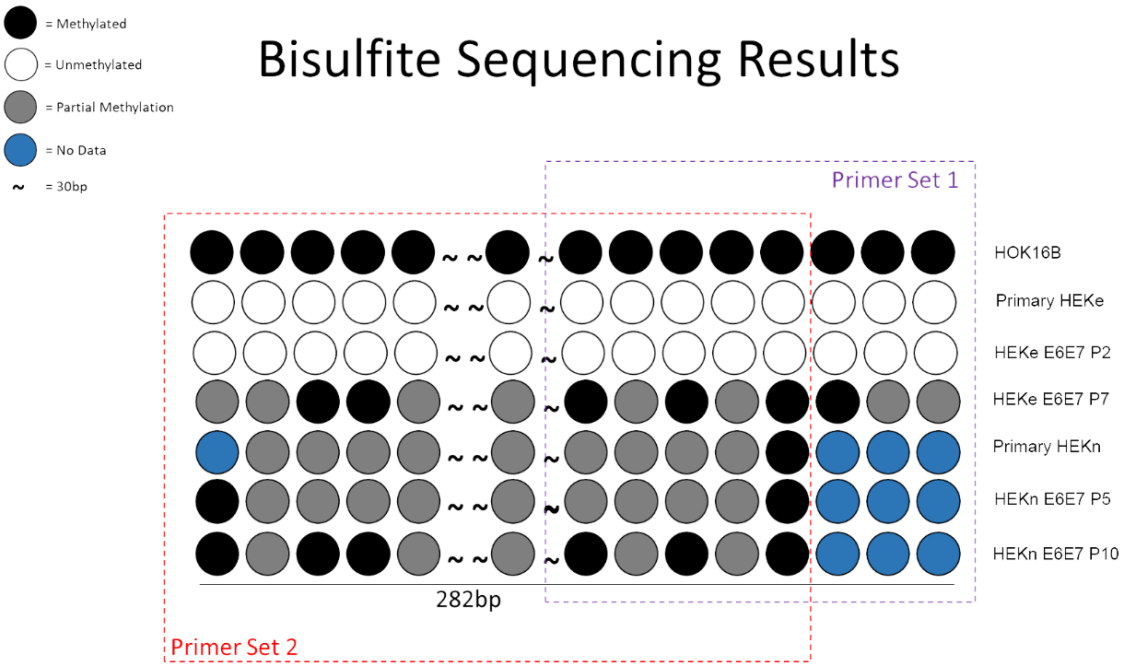

Figure 5: *Increased CDKN2A intragenic methylation is confirmed to occur at the second time point post-transduction with HPV-16 E6 and E7.* MS-HRM results for the *CDKN2A* locus was validated via bisulfite sequencing of MS-HRM products. The same overlapping primer sets were used to determine the methylation status of the 282bp region with sequencing. The HOK16B line was used as the positive control (100% methylation), and all the CpGs assayed were methylated (black circle). Primary HEKe and HEKn cells were used to set a baseline of starting methylation. All the CpGs assayed for the primary HEKe cells were unmethylated (empty circle). The sequencing results of CpGs assayed for the primary HEKn cells were a mix of fully methylated (black circle) and partially methylated (grey circle), and 4 of the CpGs assayed did not return sequencing results (blue circle). We did not detect a difference in

methylation from baseline levels at the first time point after transduction with HPV-16 *E6* and *E7* for both HEKe and HEKn lines. There was an increase in methylation at the second time point after transduction, which was expected based on the MS-HRM assay. Bisulfite sequencing confirmed that there was increase in methylated for HEKe E6E7 P7 and HEKn E6E7 P10, but there was no change in methylation at the earlier time point.

4. Discussion

Our previous tumor classification studies to distinguish HPV-positive and HPV-negative HNSCC have established that the ability to resolve optimal differences in HPV-related OPSCC tumors is dependent on the expression of HPV-16 oncogenes *E6* and *E7* [10]. Moreover, our analyses of HNSCC suggest that HPV detection in oropharyngeal tumors predicts survival, particularly for those tumors expressing HPV *E6* and *E7* [37]. There is now strong biological evidence for the role of E6 and E7 oncoproteins as the critical viral genes that cause cellular transformation and tumor induction [38]. There is also evidence of HPV-16 E6 and E7 targeting critical epigenetic modifier proteins, such as histone methyltransferases, for modulating specific gene transcription in cervical cancer [39]. Our previous studies of human HNSCC identified a 22 CpG HPV methylation panel whose methylation status distinguishes OPSCC tumors with active and latent HPV-16 infections [10]. Several of these epigenetic changes targeted the *CDKN2A* locus from which the p16(INK4a) and p14(ARF) mRNA transcripts originate. It was therefore prudent for us to test the hypothesis that observed epigenetic and transcriptional changes in the *CDKN2A* locus were specifically related to the expression of E6 and E7 oncogenic proteins, and to measure the temporal relationship observed in the downstream CG dinucleotide enriched site (CpG island) of *CDKN2A* and increased expression of p16(INK4a) and p14(ARF).

Rather than use human keratinocytes infected with the entire high risk HPV-16 virus, we specifically measured *E6* and *E7* induced DNA methylation and mRNA changes in the *CDKN2A* locus using the amphotropic retrovirus LXSN16E6E7, which encodes both the HPV-16 *E6* and *E7* open reading frames under the control of the moloney murine leukemia virus (MoMuLV) promoter-enhancer sequences. Transduced primary HEK cells expressed both HPV-16 oncogenes *E6* and *E7* as early as the first time point post-transduction (passage 2 for the HEKe E6E7 line and passage 5 for the HEKn E6E7 line), as measured by real-time PCR. This constitutive expression was maintained throughout the experimental timeline. This is not surprising as this vector has been utilized previously in the immortalization of several cell types, including epithelial cell types [40-42].

Accompanying the expression of HPV-16 oncogenes *E6* and *E7* was an increase in expression of transcripts originating from the *CDKN2A* locus. Both p14(ARF) and p16(INK4a) transcripts were dramatically increased at the earliest recorded time point (passage 2 for the HEKe E6E7 line and passage 5 for the HEKn E6E7 lines) with the highest increase observed for p16(INK4a) (Median Fold-Increase of 31.1 for the HEKe E6E7 line; **Table 3**). These expression changes observed in the HEKe E6E7 line persisted and increased through the second time point, giving transcript levels comparable to those observed in the HPV-positive HOK16B cell line. These changes likely represent an HPV oncoprotein-mediated cell cycle disruption usually observed in HPV-positive HNSCC, facilitated by the loss of Rb and the loss of

feedback inhibition and overexpression of p16(INK4a) (**Figure 1**) [38].

Also of interest were the accompanying epigenetic changes in the *CDKN2A* locus following transduction with E6 and E7 oncoproteins. Our previous work demonstrated a significant association between HPV+/p16+ oropharyngeal primary tumors and methylation of a CpG island located downstream of the promoter region in the *CDKN2A* locus (**Figure 2**) [10]. Using MS-HRM to study DNA methylation changes across the CpG island, we were able to confirm that oncogenes *E6* and *E7* alone were sufficient to induce an increase in DNA methylation across this CpG island region at the second time point post-transduction **(Figure 4)**. It should be noted that nonpromoter DNA methylation did not appear to be required for the increase in p14(ARF) and p16(INK4a) transcripts, as these changes did not begin to appear until a 25% methylation status at the later point. It is possible that DNA methyltransferases (DNMTs) are being recruited to the *CDKN2A* locus after the upregulation of transcription simply due to an open and active chromatin conformation, and active transcription or that other methylation barriers may prevent methylation from spreading to promoters [43,44].

It has been previously demonstrated that viral oncoproteins are capable of altering the methylome in tumor cells. Viral oncoproteins such as adenovirus E1A and HPV oncoprotein E7 have been shown to bind and regulate DNMT1 methyltransferase activity *in vitro* [16]. Similarly, the HPV-16 oncoprotein E6 has been shown to upregulate DNMT1 expression indirectly via the E6-mediated degradation of p53 [15]. These changes in DNMT1 activity have effects on other downstream targets critical in tumorigenic pathways, including E-cadherin and cyclin A1 [45,46], and may be responsible for the intragenic *CDKN2A* methylation we observed in this study. It is also likely that additional oncoprotein-mediated alterations in gene expression are linked to host DNA methylation [47].

In summary, our experiments demonstrate, in primary human keratinocytes, a more direct connection between expression of viral oncogenes *E6* and *E7*, and the nonpromter DNA methylation changes within the *CDKN2A* locus that accompany increase in the levels of p16(INK4a) and p14(ARF) transcripts. The expression of HPV-16 *E6* and *E7* alone were sufficient to reproduce the intragenic *CDKN2A* methylation and increased *CDKN2A* transcription signature associated with HPV-positive OPSCC. With this study, we were also able to show that intragenic *CDKN2A* methylation occurs after p14(ARF) and p16(INK4a) transcription, suggesting that *CDKN2A* gene expression is independent of methylation. Future experiments will explore whether the aberrant changes in DNA methylation observed within this CpG island may affect the binding of regulatory protein factors, or possibly alter chromatin conformation in such a way as to facilitate expression from the *CDKN2A* locus.

Acknowledgements:

This study was partially supported by National Institute of Dental & Craniofacial Research and National Cancer Institute grants (DE023941 to NFS and TJB, CA131648 to TJB, and CA115243 to NFS), and the departments of Otorhinolaryngology-Head and Neck Surgery and Pathology at Montefiore Medical Center. Thomas J. Ow's contribution was supported in part by NIH-NIDCR grant 1 K23 DE027425.

References:

1. Ang KK, Harris J, Wheeler R, et al. Human papillomavirus and survival of patients with oropharyngeal cancer. *N Engl J Med.* 2010;363(1):24-35.
2. Gillison ML, D'Souza G, Westra W, et al. Distinct risk factor profiles for human papillomavirus type 16-positive and human papillomavirus type 16-negative head and neck cancers. *Journal of the National Cancer Institute.* 2008;100(6):407-420.
3. Fakhry C, Westra WH, Li S, et al. Improved survival of patients with human papillomavirus-positive head and neck squamous cell carcinoma in a prospective clinical trial. *J Natl Cancer Inst.* 2008;100(4):261-269.
4. Ben-Dayan MM, MacCarthy T, Schlecht NF, et al. Cancer as the Disintegration of Robustness: Population-Level Variance in Gene Expression Identifies Key Differences Between Tobacco- and HPV-Associated Oropharyngeal Carcinogenesis. *Arch Pathol Lab Med.* 2015;139(11):1362-1372.
5. Chung CH, Zhang Q, Kong CS, et al. p16 protein expression and human papillomavirus status as prognostic biomarkers of nonoropharyngeal head and neck squamous cell carcinoma. *J Clin Oncol.* 2014;32(35):3930-3938.
6. Salazar CR, Anayannis N, Smith RV, et al. Combined P16 and human papillomavirus testing predicts head and neck cancer survival. *Int J Cancer.* 2014;135(10):2404-2412.
7. Pyeon D, Newton MA, Lambert PF, et al. Fundamental Differences in Cell Cycle Deregulation in Human Papillomavirus–Positive and Human Papillomavirus–Negative Head/Neck and Cervical Cancers. *Cancer research.* 2007;67(10):4605-4619.
8. Paschos K, Allday MJ. Epigenetic reprogramming of host genes in viral and microbial pathogenesis. *Trends in Microbiology.* 2010;18(10):439-447.
9. Lawrence MS, Sougnez C, Lichtenstein L, et al. Comprehensive genomic characterization of head and neck squamous cell carcinomas. *Nature.* 2015;517(7536):576-582.
10. Schlecht NF, Ben-Dayan M, Anayannis N, et al. Epigenetic changes in the CDKN2A locus are associated with differential expression of P16INK4A and P14ARF in HPV-positive oropharyngeal squamous cell carcinoma. *Cancer Med.* 2015;4(3):342-353.
11. Lleras RA, Smith RV, Adrien LR, et al. Unique DNA methylation loci distinguish anatomic site and HPV status in head and neck squamous cell carcinoma. *Clin Cancer Res.* 2013;19(19):5444-5455.
12. Sartor MA, Dolinoy DC, Jones TR, et al. Genome-wide methylation and expression differences in HPV(+) and HPV(-) squamous cell carcinoma cell lines are consistent with divergent mechanisms of carcinogenesis. *Epigenetics.* 2011;6(6):777-787.
13. Marsit CJ, Christensen BC, Houseman EA, et al. Epigenetic profiling reveals etiologically distinct patterns of DNA methylation in head and neck squamous cell carcinoma. *Carcinogenesis.* 2009;30(3):416-422.
14. von Knebel Doeberitz M, Prigge ES. Role of DNA methylation in HPV

associated lesions. *Papillomavirus Res.* 2019;7:180-183.
15. Au Yeung CL, Tsang WP, Tsang TY, Co NN, Yau PL, Kwok TT. HPV-16 E6 upregulation of DNMT1 through repression of tumor suppressor p53. *Oncol Rep.* 2010;24(6):1599-1604.
16. Burgers WA, Blanchon L, Pradhan S, de Launoit Y, Kouzarides T, Fuks F. Viral oncoproteins target the DNA methyltransferases. *Oncogene.* 2007;26(11):1650-1655.
17. Jones PA, Baylin SB. The Epigenomics of Cancer. *Cell.* 2007;128(4):683-692.
18. Jones PA. Functions of DNA methylation: islands, start sites, gene bodies and beyond. *Nat Rev Genet.* 2012;13(7):484-492.
19. Murtha M, Esteller M. Extraordinary Cancer Epigenomics: Thinking Outside the Classical Coding and Promoter Box. *Trends Cancer.* 2016;2(10):572-584.
20. Maunakea AK, Nagarajan RP, Bilenky M, et al. Conserved Role of Intragenic DNA Methylation in Regulating Alternative Promoters. *Nature.* 2010;466(7303):253-257.
21. Kempster S, Phillips WA, Baindur-Hudson S, Thomas RJS, Dow C, Rockman SP. Methylation of exon 2 of p16 is associated with late stage oesophageal cancer. *Cancer Letters.* 2000;150(1):57-62.
22. Ye X, Mo M, Xu S, et al. The hypermethylation of p16 gene exon 1 and exon 2: potential biomarkers for colorectal cancer and are associated with cancer pathological staging. *BMC Cancer.* 2018;18.
23. Spitzwieser M, Entfellner E, Werner B, et al. Hypermethylation of CDKN2A exon 2 in tumor, tumor-adjacent and tumor-distant tissues from breast cancer patients. *BMC Cancer.* 2017;17.
24. Wijetunga NA, Belbin TJ, Burk RD, et al. Novel epigenetic changes in CDKN2A are associated with progression of cervical intraepithelial neoplasia. *Gynecol Oncol.* 2016;142(3):566-573.
25. Arechederra M, Daian F, Yim A, et al. Hypermethylation of gene body CpG islands predicts high dosage of functional oncogenes in liver cancer. *Nat Commun.* 2018;9(1):3164.
26. Ben-Dayan MM, Ow TJ, Belbin TJ, et al. Nonpromoter methylation of the CDKN2A gene with active transcription is associated with improved locoregional control in laryngeal squamous cell carcinoma. *Cancer Med.* 2017;6(2):397-407.
27. Lleras RA, Adrien LR, Smith RV, et al. Hypermethylation of a cluster of Kruppel-type zinc finger protein genes on chromosome 19q13 in oropharyngeal squamous cell carcinoma. *Am J Pathol.* 2011;178(5):1965-1974.
28. Schlecht NF, Brandwein-Gensler M, Nuovo GJ, et al. A comparison of clinically utilized human papillomavirus detection methods in head and neck cancer. *Mod Pathol.* 2011;24(10):1295-1305.
29. Wojdacz TK, Dobrovic A, Hansen LL. Methylation-sensitive high-resolution melting. *Nat Protoc.* 2008;3(12):1903-1908.
30. Alam H, Sehgal L, Kundu ST, Dalal SN, Vaidya MM. Novel function of keratins 5 and 14 in proliferation and differentiation of stratified epithelial cells. *Mol Biol Cell.* 2011;22(21):4068-4078.
31. Fuchs E, Nowak JA. Building epithelial tissues from skin stem

cells. *Cold Spring Harb Symp Quant Biol.* 2008;73:333-350.
32. Watt FM. Involucrin and other markers of keratinocyte terminal differentiation. *J Invest Dermatol.* 1983;81(1 Suppl):100s-103s.
33. Wong CW, LeGrand CF, Kinnear BF, et al. In Vitro Expansion of Keratinocytes on Human Dermal Fibroblast-Derived Matrix Retains Their Stem-Like Characteristics. *Sci Rep.* 2019;9(1):18561.
34. Jones DL, Alani RM, Munger K. The human papillomavirus E7 oncoprotein can uncouple cellular differentiation and proliferation in human keratinocytes by abrogating p21Cip1-mediated inhibition of cdk2. *Genes Dev.* 1997;11(16):2101-2111.
35. Pei XF, Sherman L, Sun YH, Schlegel R. HPV-16 E7 protein bypasses keratinocyte growth inhibition by serum and calcium. *Carcinogenesis.* 1998;19(8):1481-1486.
36. Zehbe I, Richard C, DeCarlo CA, et al. Human papillomavirus 16 E6 variants differ in their dysregulation of human keratinocyte differentiation and apoptosis. *Virology.* 2009;383(1):69-77.
37. Salazar CR, Smith RV, Garg MK, et al. Human papillomavirus-associated head and neck squamous cell carcinoma survival: a comparison by tumor site and initial treatment. *Head Neck Pathol.* 2014;8(1):77-87.
38. Faraji F, Zaidi M, Fakhry C, Gaykalova DA. Molecular mechanisms of human papillomavirus-related carcinogenesis in head and neck cancer. *Microbes Infect.* 2017;19(9-10):464-475.
39. Hsu CH, Peng KL, Jhang HC, et al. The HPV E6 oncoprotein targets histone methyltransferases for modulating specific gene transcription. *Oncogene.* 2012;31(18):2335-2349.
40. Tsao SW, Mok SC, Fey EG, et al. Characterization of human ovarian surface epithelial cells immortalized by human papilloma viral oncogenes (HPV-E6E7 ORFs). *Exp Cell Res.* 1995;218(2):499-507.
41. Johnson GA, Burghardt RC, Newton GR, Bazer FW, Spencer TE. Development and characterization of immortalized ovine endometrial cell lines. *Biol Reprod.* 1999;61(5):1324-1330.
42. Hung SC, Yang DM, Chang CF, et al. Immortalization without neoplastic transformation of human mesenchymal stem cells by transduction with HPV16 E6/E7 genes. *Int J Cancer.* 2004;110(3):313-319.
43. Turker MS. Gene silencing in mammalian cells and the spread of DNA methylation. *Oncogene.* 2002;21(35):5388-5393.
44. Issa JP. CpG island methylator phenotype in cancer. *Nat Rev Cancer.* 2004;4(12):988-993.
45. Laurson J, Khan S, Chung R, Cross K, Raj K. Epigenetic repression of E-cadherin by human papillomavirus 16 E7 protein. *Carcinogenesis.* 2010;31(5):918-926.
46. Chalertpet K, Pakdeechaidan W, Patel V, Mutirangura A, Yanatatsaneejit P. Human papillomavirus type 16 E7 oncoprotein mediates CCNA1 promoter methylation. *Cancer Sci.* 2015;106(10):1333-1340.
47. Na Rangsee N, Yanatatsaneejit P, Pisitkun T, Somparn P, Jintaridth P,

Topanurak S. Host proteome linked to HPV E7-mediated specific gene hypermethylation in cancer pathways. *Infect Agent Cancer.* 2020;15:7.

